An Alternative Approach to Reduced-Complexity CPM-Receivers

JOHANNES HUBER, MEMBER, IEEE, AND WEILING LIU, STUDENT MEMBER, IEEE

Abstract—**Optimum coherent receivers for CPM-signals have in general a high degree of complexity. Especially for the most interesting schemes that offer significant power and bandwidth efficiency with smoothed frequency pulses, or that implement an additional convolutional code, the number of parallel filters at the receiver input, and the number of memory-states which have to be traced by a Viterbi-decoder, both become increasingly large. In contrast to a previous approach dealing with the receiver's complexity each one of these problems is treated separately in this paper. For this purpose, a concise analysis of the inherent trellis-encoder associated with CPM is initially given. It is then demonstrated that for almost all schemes of interest in practice, it is quite sufficient for the receiver to implement only four or six linear filters which respresent proper reference signals. For a reduction in the number of memory-states, decision feedback sequence estimation together with a minimization of the unprocessed intersymbol interference is proposed. Modifications of this procedure allow a state-reduction without, or with only negligible losses, because only error events with large distances are affected. Combinations of these methods make possible an almost continuous tradeoff between receiver-complexity and SNR-losses. Several examples are considered for which evaluations of minimum Euclidean distances and results obtained by simulation are given.**

I. INTRODUCTION

THE use of continuous phase modulation (CPM [1]–[3]) in digital communication systems offers power and bandwidth efficiency advantages, when compared to more traditional modulation schemes. The main nonlinear effects of high power amplifiers, i.e., AM/AM- and AM/PM-conversion (cf. [4]), are avoided by systems utilizing CPM, due to the constant signal envelope. Therefore, efficient signal amplification without a significant reconstruction of undesired spectral sidelobes is possible. The CPM-signal contains an inherent trellis code due to the phase continuity condition and the correlative coding of smoothed frequency pulses. Both effects are appropriate for a reduction of signal bandwidth and transmitter power requirements. The penalty for the advantages offered by CPM in general is a highly complex coherent receiver implementing a maximum likelihood sequence estimation algorithm. That is, a large number of parallel linear filters is necessary at the receiver input, and many memory-states have to be traced by a Viterbi-decoder ([1]–[3], [31]).

Manuscript received May 2, 1988; revised December 23, 1988. This work was supported by the Deutsche Forschungsgemeinschaft under Contract Tr 160/5-2 and Tr 160/5-3. This paper was presented in part at GLOBECOM '87 and ICC '88.

The authors are with the Institute for Communication Engineering, University of the Federal Armed Forces, Munich, West Germany.

IEEE Log Number 8928623.

Much work (e.g., [1], [5]–[10], [38]–[39]) has been done to overcome some of the realization problems associated with coherent CPM receivers. For the special case of binary CPM with modulation index $1/2$, simple MSK-type receivers can be used with only small losses when compared to the performance of the optimum receiver. For other CPM-schemes, a complexity reduction was proposed in [1], [6] by the use of a slightly mismatched receiver. That is, shorter frequency pulses are used at the receiver than at the transmitter, resulting in both the number of linear filters and memory-states to be reduced in one step.

In contrast to this approach for reducing the receiver complexity we treat both issues separately in this paper. For that purpose, an analysis of the inherent trellis-encoder of CPM is presented in Section II. In order to study the question, how many dimensions are necessary per symbol interval to accurately represent a CPM-signal in a signal space, we make use of a bound on the maximum number of time-limited orthogonal functions constrained to a given frequency bandwidth. Especially for partial response frequency pulses [2], an extensive reduction in the number of required linear filters is predicted by this method. The selection of a small number of reference signals is based on two simple proposed methods. One such method involves the application of a modified Gram–Schmidt procedure to the set of signal segments within one modulation interval, while the second requires the introduction of a few simple functions to form a signal space, in which the Euclidean distances between all signal elements are represented very accurately. The results presented in Section III show that four or six dimensions are sufficient to yield good performance results for reduced complexity receivers in most CPM-schemes of interest in practice.

For the problem of an excessive number of different memory-states, the use of different reduced-state sequence estimation algorithms is proposed in Section IV. Starting from decision feedback sequence estimation ([14], [15]) modified versions are developed to minimize the loss of minimum Euclidean distance at several levels of complexity reduction.

The complexity reduction method using shorter frequency pulses at the receiver than at the transmitter [1], [6] may be interpreted as a special case of the alternative approach presented in this paper. The separate treatment of both problems yields a more significant reduction in

0733-8716/89/1200-1437$01.00

the number of receiver filters, and smaller SNR-losses have to be tolerated because of the use of decision feedback.

II. Inherent Trellis Code of CPM

A discussion on the receiver complexity reduction requires a short analysis of the inherent trellis code of CPM. This decomposition of CPM was derived in [16], [17]. The independent and more general approach used by Rimoldi [18], yielded similar results.

At first, we use a notation similar to [1]–[3] for CPM-signals, namely,

$$s(t, \alpha) = \sqrt{2E/T} \cos\left(\Phi(t, \boldsymbol{\alpha})\right) \tag{1}$$

with the phase function

$$\Phi(t, \boldsymbol{\alpha}) = 2\pi f_o t + 2\pi h \sum_{i=0}^{\infty} \alpha_i q(t - iT) \tag{2}$$

where E denotes the signal energy per modulation interval T, f_o is the carrier frequency, and $h = k/p$ denotes the rational modulation index where k and p are relatively prime integers. Normally, the data sequence is mapped to M-ary bipolar phase-increments, that is $\alpha_i \in \{\pm 1, \pm 3, \cdots \pm(M-1)\}$ where M is assumed to be even.

The phase pulse $q(t)$ is normalized in the sense that

$$q(t) = \begin{cases} 0 & t \leqq 0 \\ 1/2 & t > LT \end{cases}. \tag{3}$$

The frequency pulse $g(t) = \dot{q}(t)$ occupies L intervals each of duration T (cf. [1]).

Within the time interval $nT \leqq t < (n+1)T$, for $n > L$ the phase-function is expressed by

$$\Phi(t, \boldsymbol{\alpha}) = 2\pi f_o t + \Theta_{n-L} + 2\pi h \sum_{i=n-L+1}^{n} \alpha_i q(t - iT). \tag{4}$$

For modulation indexes with an odd numerator k, the elements

$$\Theta_{n-L} = \frac{\pi}{p}\left(\left(k \sum_{i=0}^{n-L} \alpha_i\right) \bmod 2p\right) \tag{5}$$

of the sequence $\boldsymbol{\Theta}$ of phase-states belong to two different classes, as the sum $\Sigma\ \alpha_i$ alternatively is even and odd. Therefore, the Markov chain of phase-states has $2p$ states, a period of 2, and in this case is reducible (cf. [19]).

In order to generate an irreducible ergodic Markov chain of modified phase-states Ψ_{n-L} in any case, we make use of a slope-function $c(t)$, defined by

$$c(t) \triangleq \begin{cases} 0 & t < 0 \\ \dfrac{M-1}{2LT}\, t & 0 \leqq t < LT \\ (M-1)/2 & t \geqq LT \end{cases}$$

and add a zero term to (4) so that for $n > L$

$$\begin{aligned} \Phi(t, \alpha) &= 2\pi f_o t + 2\pi h \sum_{i=0}^{n} \left(\alpha_i q(t - iT) \right. \\ &\qquad \left. + c(t - iT) - c(t - iT)\right) \\ &= 2\pi f_R t + \varphi_{oR} + \frac{2\pi}{p} \Psi_{n-L} \\ &\qquad + 2\pi h \sum_{i=n-L+1}^{n} b(t - iT, \beta_i). \end{aligned} \tag{6}$$

For $t > LT$, the information carrying phase is defined relative to a reference phase, namely,

$$2\pi f_o t - 2\pi h \sum_{i=0}^{\infty} c(t - iT) = 2\pi f_R t + \varphi_{oR}$$

where the reference frequency f_R, defined by

$$f_R \triangleq f_o - h\frac{M-1}{2T}, \tag{7}$$

is identical to the instantaneous signal frequency corresponding to a long sequence $\alpha_i = -(M-1)$ for certain CPM schemes.

We introduce unipolar phase-increments β_i where

$$\beta_i = (\alpha_i + M - 1)/2 \in \{0, 1, \cdots, (M-1)\}, \tag{8}$$

so that the phase transitions are expressed by

$$b(t, \beta) = \left(2\beta - (M-1)\right) q(t) + c(t) \tag{9}$$

with the modified phase states given by

$$\Psi_{n-L} = \left(k \sum_{i=0}^{n-L} \beta_i\right) \bmod p \in \{0, 1, \cdots, (p-1)\} \tag{10}$$

which are updated recursively according to

$$\Psi_n = (\Psi_{n-1} + k\beta_n) \bmod p. \tag{11}$$

From the definition of the phase transition function $b(t, \beta)$, the unipolar description of a CPM-signal relative to the reference frequency f_R, which often was used for schemes utilizing rectangular frequency pulses (e.g., [20], [31]), is hereby extended to schemes with arbitrary frequency pulses.

The CPM-modulator can now be divided into a "natural" trellis encoder with memory and a mapper or signal-table [36], which associates signal segments of duration T to the encoder output. The structure of the inherent trellis encoder shown in Fig. 1 is immediately derived from (6) and (11). The memory due to the intersymbol interference (ISI) associated with the frequency pulses is represented by a M-ary shift register with $L-1$ stages. The memory introduced by the continuous phase condition has a recursive structure due to (11). This recursive structure corresponds to the well-known differential encoder used

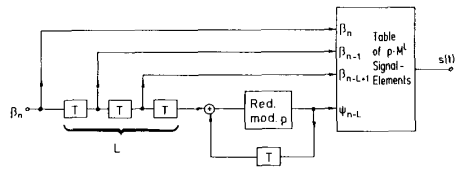

Fig. 1. Decomposition of a CPM-modulator into a trellis encoder and a table of signal elements.

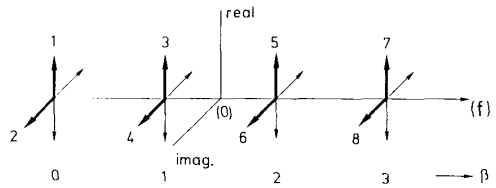

Fig. 2. Graphic representation of the signal elements ($M = 4$, $h = 1/4$) (The in-phase and quadrature representor are highlighted by bold face lines.)

for the transformation of PSK to DPSK and originates from the mapping of the data to phase-increments. Its application to the phase-state sequence generates the rotational invariance property of CPM. As for any phase modulation technique, a mapping of the data to the absolute phase is also possible. For $M = p$ the information can be expressed by the signal phase at the end of the corresponding interval and therefore is called a phase-state mapping [17]. (Phase and frequency change their roles as master and slave when compared to the usual phase-increment mapping.) For $M = p^{\mu}$; $\mu \in \boldsymbol{N}$, a semidifferential mapping has been proposed in [18]. For such an absolute phase-mapping, the continuous phase condition is represented by only one p-ary delay element. The resulting nonrecursive structure of the natural trellis encoder offers some advantages when convolutional codes are combined with CPM, in that more delay elements can be shared by both encoders. A state reduction is therefore possible however at the price of losing the rotational invariance property [16], [17].

Since all $p \cdot M^L$ different signal segments form the elements of the signal set, the rate of the inherent trellis encoder is equal to $\log(M)/(L \cdot \log(M) + \log(p))$. In Fig. 2, a graphic illustration for the elements of the signal set is given for $L = 1$. The phase-state is represented by the angle within a complex plane at a specific phase-increment β. Since a certain transition of the instantaneous frequency is associated with a specific phase increment, this illustration may also be interpreted along the frequency axis (not to be confused with the signal spectra!). (Complex baseband equivalents of the bandpass signal elements and the condition $f_o >> Mh/T$ will be used in the sequel). Since all signal elements in one complex plane are related to the same information, this figure again elucidates the rotational invariance property of CPM with phase-increment mapping.

III. Reduction of the Number of Linear Filters

Due to the nonlinear modulation process, only those signal elements which are addressed by identical phase-increments β_i; $i \in \{n - L + 1, \cdots, n\}$, but by different phase-states Ψ_{n-L}, can be expressed by linear combinations. All such signal elements are representable by two representors having the phase states $\Psi_{n-L} = 0$ and $\Psi_{n-L} = p/4$ (in-phase- and quadrature components; $p/4 \in \boldsymbol{R}$). In Fig. 2 the representative signal elements are highlighted with boldface lines. In general, $2 \cdot M^L$ (M^L for $p \leqq 2$) linear filters or correlators appear to be necessary at the receiver input in order to generate a sufficient statistics of the received signal under additive white Gaussian noise (AWGN) interference conditions (cf. [1], [2], [3]).

The number of necessary such linear filters is closely related to the answer of the question, how many orthogonal time-limited functions exist whose spectra are concentrated within a certain bandwidth $[-W, +W]$? This difficult problem has been intensively analyzed (e.g., [12], [13]), with a condensed presentation to be found in [11] chapter 5.

For CPFSK or CPM with sufficiently smoothed frequency pulses ($L \geqq 3$) the phase-functions within one time interval T are straight lines or slight variations of these. Therefore the real and imaginary parts of the spectra of all $2 \cdot M^L$ representative signal-elements can roughly be approximated by $\sin(\pi(f - f_j)T)/(\pi(f - f_j)T)$ functions for $j \in \{1, \cdots, M^L\}$. In Fig. 3, the real part of such spectra is illustrated. For frequency pulses $g(t) \geqq 0$; $\forall t$, the center frequencies f_j of the baseband equivalents of the signal elements are concentrated within the interval

$$f_j \in \left[-(M-1)\frac{h}{2T}, +(M-1)\frac{h}{2T}\right]. \tag{12}$$

Therefore, in the most extreme case, less than 10 percent of the energy of any signal element is outside the bandwidth $[-W, +W]$, [11] where

$$W = (M-1)\frac{h}{2T} + \frac{1}{T}. \tag{13}$$

The number D of time-limited orthogonal functions, which meet this condition is bounded, that is $D \leqq D_{\max}$ with (ref. to [11] p. 294 footnote)

$$\begin{aligned} D_{\max} &= 2 \cdot \lceil 2.22WT \rceil \\ &= 2 \cdot \lceil 1.11 \cdot h(M-1) + 2.22 \rceil \\ \lceil x \rceil &= \text{largest integer} < x + 1. \end{aligned} \tag{14}$$

Therefore, all signal-elements are representable by an appropriate set of at most $D_{\max}$ real functions, so that quite sufficient statistics associated with a segment of the received signal having duration T, can be obtained with D

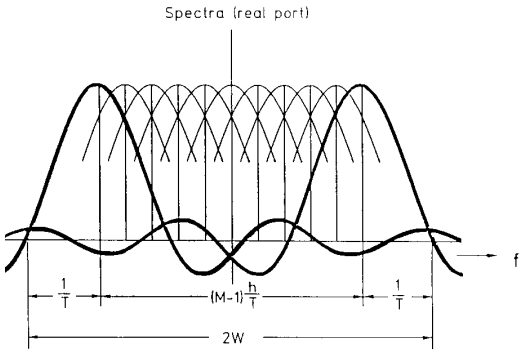

Fig. 3. Approximation of the spectra (real part) of the signal elements.

$= \min(D_{\max}, 2M^L)$ linear filters. (The factor 2 in (14) originates from the presence of complex signal elements.) According to (14), at least six, (for $h \cdot (M-1) > 0.7$ eight) dimensions are required. The applicability of MSK-type receivers to binary CPM with $h = 1/2$ shows this bound to be conservative. However the main result of the rough estimate provided by (14) is that in spite of the nonlinear ISI, the number of linear filters needs not to increase exponentially with the duration L of the frequency pulses. The problem of finding appropriate reference signals remains unsolved, with an optimum solution perhaps possible by application of the theory developed in [12], [13] (cf. [23]). Here, we propose two simple approaches.

The first approach involves transforming the $2 \cdot M^L$ representative signal elements into a signal space with rectangular (Cartesian) coordinates. The reference-signals are then searched within the set of the signal elements. A computer program was written to implement the Gram–Schmidt procedure in which the correlation coefficients of all pairs of signal elements are used. These correlation coefficients can be easily calculated for rectangular frequency pulses ($L = 1$: 1REC, see, e.g., [20], [24]) and were evaluated by numerical integration for other frequency pulses. In this procedure, new dimensions are generated until the unit energy of all signal elements is achieved within an error of less than 10^{-8}. Although the resulting signal space always is identical, the components of the signal-vectors are quite different when the elements are differently ordered at the start of the Gram-Schmidt procedure [11]. For a reduction in the number of dimensions, we desire components which decrease as steeply as possible for higher order dimensions. This property can be achieved by a good choice in the direction of the orthonormal functions. In order to find a Cartesian basis with proper directions, we propose a Gram–Schmidt-procedure which incorporates a minimization-algorithm. The procedure starts with a given signal element and at each subsequent step a signal element is selected in such way that it has a minimum correlation with all orthogonal functions already determined. This way, the first signal space dimensions contain most of the energy, and a strong decrease in higher order dimensions is established. The starting element has to be also optimized for a steepest energy decrease. To give an example, Table I lists the maximum energy contents in the components of all vectors, which represent the signal elements of the scheme with the parameters $M = 4$, $h = 1/4$, 1REC in a Cartesian signal space. The coordinates differ only slightly from the last four dimensions. Therefore, these higher order coordinates are almost irrelevant [11] and may be omitted without significant losses. (Surprisingly, in this example the steepest energy descent was obtained by starting the procedure with one of the "inner" signal elements 3, 4, 5, 6; see Fig. 2.)

TABLE I
MAXIMUM SQUARED COMPONENTS OF THE VECTORS REPRESENTING THE SIGNAL-ELEMENTS IN A SIGNAL SPACE OVER ORTHOGONAL FUNCTIONS. (GRAM-SCHMIDT PROCEDURE INCLUDING A SELECTION ALGORITHM, CPM: $M = 4$, $h = 1/4$, 1REC)

i-th dimension i	maximum energy content
1	1
2	1
3	0.90090
4	0.90090
5	$4.1869 \cdot 10^{-2}$
6	$4.1869 \cdot 10^{-2}$
7	$6.6090 \cdot 10^{-3}$
8	$6.6090 \cdot 10^{-3}$

The losses caused by a reduction in the number of dimensions were calculated for some CPM-schemes using a sequential algorithm similar to the one described in [2] for determining the minimum Euclidean distance of a trellis-coded scheme. The utilizable Euclidean distances between all signal elements within the reduced signal space are used in place of the real distances. (The reduction in the number of dimensions causes only information loss with no introduction of unprocessed intersymbol interference. The minimum Euclidean distance can be therefore calculated in this simple way, [6].)

For some examples the losses of minimum Euclidean distance due to a reduction to four and six in the number of linear filters are listed in Table II. The results are given for CPM, both with and without the use of an additional convolutional encoder, ref. to [17], [25]. A detailed analysis of the results presented, reveals that remarkable distance losses for some specific pairs of signal elements affect only slightly the minimum Euclidean distance of the related modulation scheme. These losses are partly offset by the inherent trellis-code of a CPM-scheme, making the losses smaller when the minimum distance error events are extended over a larger number of intervals by an encoder with more memory. Especially for schemes with smoothed frequency pulses, a dramatic reduction in the

TABLE II
LOSSES OF MINIMUM EUCLIDEAN DISTANCE [IN dB] DUE TO A REDUCTION IN THE NUMBER OF DIMENSIONS TO 4 OR 6, RESP., (GRAM-SCHMIDT PROCEDURE)

number of dimensions	M=4, h=1/4, 1REC $2 \cdot M^L = 8$ dim		M=8, h=1/8, 1REC $2 \cdot M^L = 16$ dim		M=4, h=1/4, 2RC $2 \cdot M^L = 32$ dim		M=4, h=1/4, 3RC $2 \cdot M^L = 128$ dim	
	without convolutional encoder	convolutional encoder (13,6)	without convolutional encoder	convolutional encoder (2,1), $R_c = 2/3$	without convolutional encoder	convolutional encoder (13,6)	without convolutional encoder	convolutional encoder (2,1)
4	0.25	0.06	0.52	0.31	0.24	0.17	0.16	0.18
6	~0	~0	0.01	0.01	0.01	~0	0.01	~0

number of required linear filters while incurring very low losses is possible. A smaller number of dimensions is required in practice than theoretically predicted by the bound (14).

The receiver needs only implement correlators for the first D signal elements selected by the Gram–Schmidt procedure. If metrics expressed in terms of Euclidean distances are preferred, calculations may be simplified by a transformation of the correlator output samples into a Cartesian signal space via a matrix B, whose elements b_{jk}; $j, k \in \{0, \cdots, D-1\}$ are the coefficients of the orthonormal functions generated by the Gram–Schmidt procedure. For metrics expressed in terms of correlations this transformation is not necessary.

There are two disadvantages associated with this method of selecting the reference signals. The first D selected reference signals need not be symmetrical with respect to the carrier frequency by the procedure. Therefore using quadrature demodulation together with complex baseband signal processing, more than D real filters may have to be implemented [1], [2], [3]. (In the examples considered, the first 4 signal elements were always chosen symmetrically with respect to the carrier frequency, while for $D > 4$, this condition was not satisfied.) On the other hand, the best coordinate directions may not be obtained by this method. To illustrate this point we use the simple example of a dimensionality reduction from 2 to 1. In Fig. 4, three signal elements are represented by x marks. Based on the proposed procedure, only such one-dimensional spaces (straight lines) which are defined by the origin and one of the signal points x would be taken into consideration. For highly noise immune modulation schemes, it is not the energy of the signal elements but rather their distances that must be accurately represented in a signal space. Therefore, if we take a new signal element marked by 0 as reference which is not within the original set, an improved representation of these distances may be possible. Based on these considerations, in our second approach we introduce new reference signals which are taken symmetrically with respect to the carrier frequency and equally spaced on the frequency axis. For an even number

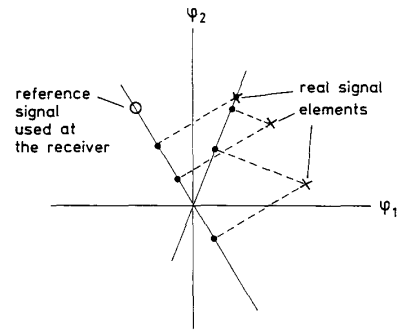

Fig. 4. Projection of the distances between signal elements marked by x to a reference-signal marked by 0 which is not an element of the signal set.

D of dimensions we define the set of reference signal elements $\{e_j(t)\}$ to be

$$e_j(t) = \begin{cases} \cos\left(2\pi t\left(f_o + \frac{\Delta f}{2}(j + 1 - D/2)\right)\right); \\ \quad j \text{ even} \\ -\sin\left(2\pi t\left(f_o + \frac{\Delta f}{2}(j - D/2)\right)\right); \\ \quad j \text{ odd} \end{cases}$$

$$t \in [0, T)$$

$$j \in \{0, 1, \cdots, (D-1)\};\ D \geqq 2;\ D \text{ even}. \quad (15)$$

For a particular modulation scheme, the frequency spacing parameter Δf has to be optimized with respect to the minimum utilizable Euclidean distance. Fig. 5 illustrates the equivalent baseband reference signal elements for the cases in which 4 and 6 dimensions are used. Signals with amplitude- and/or phase-modulation and unequal frequency spacing may be slightly better in some cases, however the definition (15) is more practicable, as only one parameter needs to be optimized.

As an example, Fig. 6 shows the Euclidean distance loss as a function of the frequency spacing parameter Δf due to the use of 4 and 6 dimensions instead of $2 \cdot M^L = 128$ dimensions. The losses can be seen to be very low in the broad region corresponding to $0 < \Delta f < 1/T$. Using four dimensions and the optimized frequency spacing parameter, this loss is reduced by 31 percent when compared to the value presented in Table II. (The losses were determined by the above described method.)

In Figs. 7–10 the losses due to the use of only four or six filters with optimized frequency spacing parameters Δf are presented for several 4- and 8-ary CPM-schemes. All discrete calculated points have been connected by straight lines. For rectangular frequency pulses (1REC: CPFSK) the plots of the loss versus h display extreme fluctuations. For an interpretation of this fact, we consider the special case $M = 4$; $h = 1/3$; 1REC. This

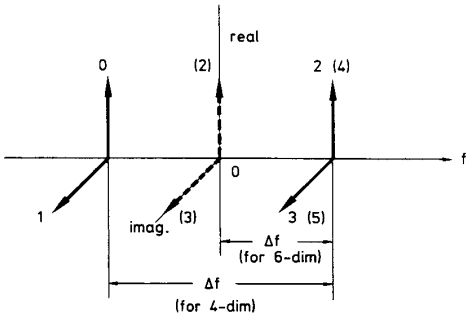

Fig. 5. Graphic representation of the reference signals (15) for 4 and 6 dimensions.

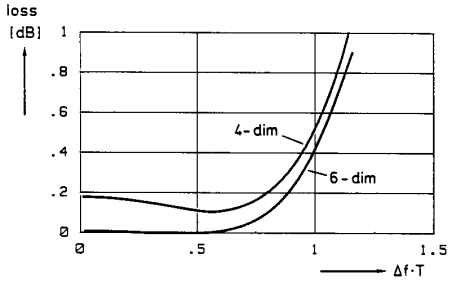

Fig. 6. Loss of minimum Euclidean distance due to a reduction of linear filters to 4 or 6, resp., as a function of the frequency spacing parameter Δf. ($M = 4$, $h = 1/4$, $3RC$, $2 \cdot M^L = 128$).

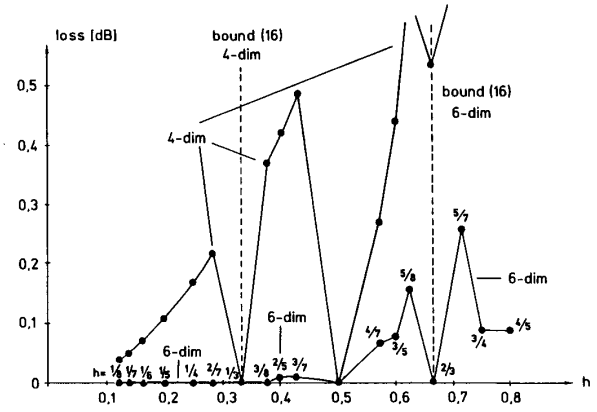

Fig. 7. Loss of minimum Euclidean distance of 4-ary schemes with different modulation indexes, 4 or 6 dimensions, Δf optimized, frequency pulses: 1REC.

scheme experiences no distance losses when four dimensions instead of $2 \cdot M^L = 8$ are used with the optimum frequency spacing parameter $\Delta f = 1/T$. The four reference-signals are matched to the "outer" signal elements ($\beta = 0$, $\beta = 3$) while for the "inner" signal elements ($\beta = 1$, $\beta = 2$) of the 4-ary scheme, no specific reference-signals exist causing mismatches to occur. Since the minimum distance error events of this scheme consists of parallel transitions in the trellis differing from the "outer" signal elements, the losses are related to high distance error events. Since for $L = 1$ there are only few signal elements, such situations exist at some isolated points. For smoothed frequency pulses many slight mismatches occur. Therefore, the curves in Fig. 9 can be seen to in-

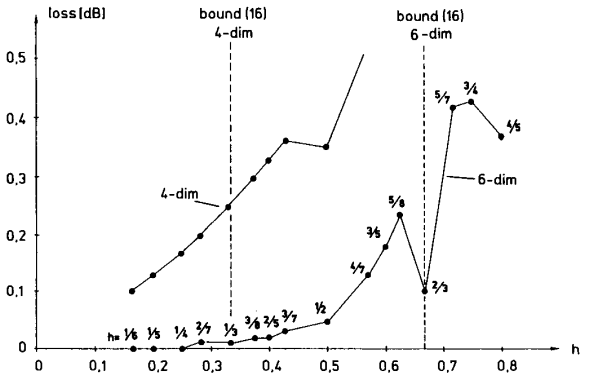

Fig. 8. Loss of minimum Euclidean distance of 4-ary schemes with different modulation indexes, 4 or 6 dimensions, Δf optimized, frequency pulses: $2RC$.

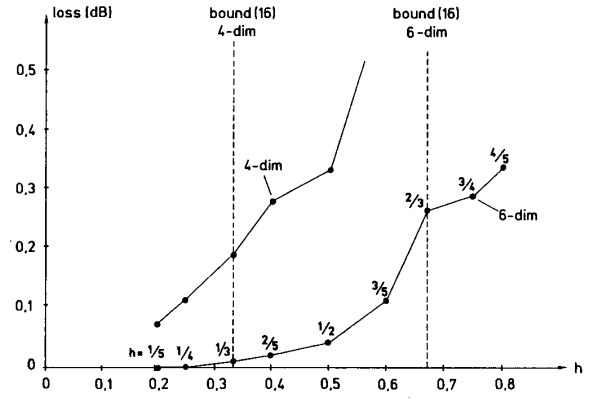

Fig. 9. Loss of minimum Euclidean distance of 4-ary schemes with different modulation indexes, 4 or 6 dimensions, Δf optimized, frequency pulses: $3RC$.

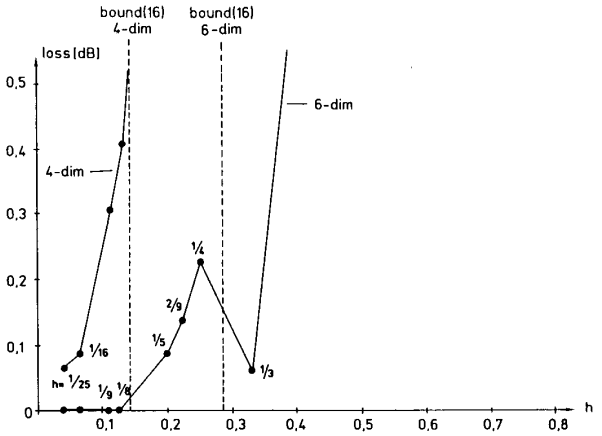

Fig. 10. Loss of minimum Euclidean distance of 8-ary schemes with different modulation indexes, 4 or 6 dimensions, Δf optimized, frequency pulses: 1REC.

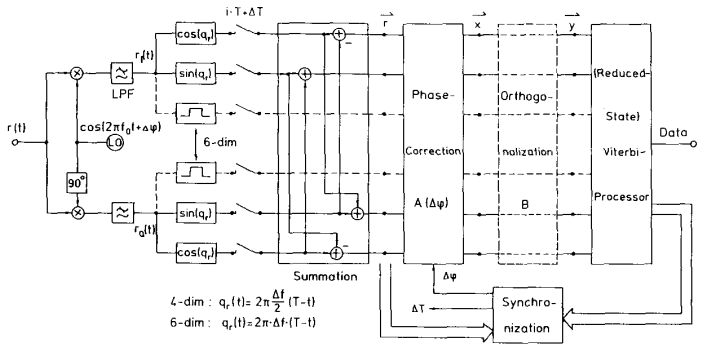

Fig. 11. Block diagram of a coherent CPM receiver with 4 or 6 dimensions.

crease monotonically. The curves in Figs. 7–10 indicate that the losses are small provided that a frequency spacing of the reference-signal elements greater than $1/T$ is not necessary to cover the "outer" signal elements on the frequency axis. These observations may be supported with a lower bound on the number of dimensions necessary when using equal spaced reference signals (15)

$$D \geqq 2 \cdot \lceil h(M-1)+1 \rceil . \tag{16}$$

If a receiver with quadrature demodulation and complex baseband signal processing is realized [1], [2], the receiver structure of Fig. 11 can be used with 4 or 6 dimensions. As the reference-signals (15) are chosen symmetrically with respect to the carrier frequency, no additional filters for in-phase and quadrature components [3] are necessary. The summation network establishes the correlation of the received signal with the complex baseband equivalents of the bandpass reference signal (15), cf. [3]. If decision aided synchronization with a free-running local oscillator ($L0$) is used [27], a phase correction $\Delta\varphi$ of the vector $\vec{r}$ consisting of the outputs of the summation network is possible by a linear transformation which is an extension of that associated with PSK or QAM receivers, namely,

$$\vec{x} = \vec{r} \cdot A(\Delta\varphi_i). \tag{17}$$

The $D \times D$ transformation matrix A [with reference-elements ordered by (15)] is given by

$$A(\Delta\varphi) = \begin{bmatrix} \cos\Delta\varphi & -\sin\Delta\varphi & 0 & 0 & 0 & 0 \\ \sin\Delta\varphi & \cos\Delta\varphi & 0 & 0 & 0 & 0 \\ 0 & 0 & \cos\Delta\varphi & -\sin\Delta\varphi & 0 & 0 \\ 0 & 0 & \sin\Delta\varphi & \cos\Delta\varphi & 0 & 0 \\ 0 & 0 & 0 & 0 & \cos\Delta\varphi & -\sin\Delta\varphi \\ 0 & 0 & 0 & 0 & \sin\Delta\varphi & \cos\Delta\varphi \end{bmatrix} . \tag{18}$$

Using this transformation, a robust decision-aided carrier phase synchronization is possible for CPM schemes via a straightforward extension of the method proposed in [28] for two-dimensional modulation schemes. The phase differences $\Delta\varphi_i$ are estimated by comparing the sequence of vectors $\vec{r}_i$ which represent the segments of the received signal with the sequence of vectors of those signal elements, which correspond to a preliminary estimate of the data sequence. (The ambiguity of the carrier phase caused by the use of a phase-state trellis with p states [eq. (10)] instead of a time variant phase-state trellis with $2p$ states [1] representing a reducible Markov chain, is easily resolved by this synchronization method.)

An algorithm for symbol synchronization may also be implemented using these vector sequences. (An approach to symbol synchronization similar to that presented in [21], requires no special equipment to generate the derivative of the received signal, because pairs of the reference signals (15) are invariant relative to differentiation operation.)

By a further (time invariant) linear transformation, rectangular coordinates may be generated that simplify metric calculations in terms of Euclidean distances (Fig. 11). The corresponding transformation matrix B can easily be determined by an application of the Gram-Schmidt-procedure on the reference signal elements (15).

Clearly, this second transformation is unnecessary when metrics expressed in terms of correlations are used or when orthonormal reference signals $e_j'(t); j \in \{0, \cdots, D-1\}$ are chosen. Such reference signals may be constructed by linear superpositions of the signals $e_j(t)$ given in (15), so that the orthonormal basis $\{e_j'(t)\}$ can be ex-

pressed in vector notation as

$$\vec{e}'(t) = \vec{e}(t) \cdot B. \tag{19}$$

However, within the Cartesian signal space, the synchronization is more complicated than in the oblique coordinate systems given by (15). Therefore the structure shown in Fig. 11 appears to be more advantageous.

An effect surprising in the first instance is apparent from Fig. 6, in that the losses due to the basis $\{e_j(t)\}$ (15) increase negligibly, when the frequency spacing parameter Δf approaches zero, whereas for $\Delta f = 0$ (two dimensions) a loss of 1.75 dB occurs. This fact can be interpreted by an analysis of the orthonormal functions $e_j'(t)$. For small (but positive) values of Δf, some functions $e_j'(t)$ are obtained by high amplification of the small differences between the functions $e_j(t)$. As the functions $e_j'(t)$ are orthogonal, they always occupy approximately the same bandwidth, independent of the original frequency spacing parameter $\Delta f (0 < \Delta f < 1/T)$. Thus, the signal elements are representable with sufficient accuracy even by such a degenerated basis that results when $\Delta f \to 0$. Clearly, a high sensitivity to the reference signals and numerical problems associated with the metric computations appear if the frequency spacing parameter Δf is chosen to be too small.

IV. Reduction in the Number of Memory States

The number of different memory-states $Z = M^{L-1} \cdot p$ of a CPM modulator (cf. Fig. 1) increases significantly, if smoothed frequency pulses ($L > 1$) and $M >$ 2-ary schemes are used and/or additional convolutional codes are applied. But such schemes are the most interesting due to power and bandwidth efficiency (see [1], [17], [24], [25], [26]). A maximum likelihood sequence estimation using the Viterbi algorithm [31] in which all possible paths through the encoder-modulator trellis are traced, becomes enormously complex.

In this paper, the complexity of a sequence-estimation procedure is measured by the number A of trellis branches, which have to be processed per equivalent bit interval [29], [30]. If a convolutional encoder with rate $R_c = u/n$ is used ($R_c = 1$: no code used), whose redundancy is transmitted by means of an increased signal space ($M = 2^n$), this complexity number A is given by

$$A = Z \cdot \frac{M^{R_c}}{R_c \log_2 (M)}$$

where Z is the number of encoder-modulator memory states.

For κ-fold multiple trellis-coded schemes ([22], [29], [30]) with κ modulation intervals for one coding interval the complexity number becomes

$$A = Z \cdot \frac{M^{\kappa R_c}}{\kappa R_c \log_2 (M)}.$$

The receiver complexity problem arising from the large number of memory-states can be diminished by an application of well-known reduced state sequence-detection algorithms, which were originally developed for signals with severe linear intersymbol interference. Such algorithms may be separated into two classes, the first of which is characterized by a forward looking procedure along a few paths with high probability and is closely related to the so-called M-algorithm (e.g., [32], [33]). The second class consists of approaches derived from the Viterbi algorithm and is characterized by looking backward for the best paths leading to states.

In this section, we discuss algorithms of the second class, especially the application of reduced state sequence estimation (RSSE) proposed in [15], [35] to CPM and some extensions of this procedure. A comparison of these methods with a search algorithm of the first class will be given at the end of this section.

At first we take a special case of RSSE, namely decision feedback sequence estimation (DFSE, [14], [15]). DFSE is only applicable if the encoder-modulator trellis has a butterfly structure. That is, the set of states must be partitionable into classes in such a way that each class comprises $M^{\kappa R_c}$ states, and all branches which emerge from these states lead to $M^{\kappa R_c}$ different successor states. An encoder with shift register memory always produces a trellis with a butterfly structure, however for CPM this property is not essential because of the recursive structure of the inherent trellis encoder (e.g., $M = 2$, $L = 1$, $h = 1/3$). For DFSE, at a first state reduction level, all states of a class (butterfly) are regarded as one hyperstate of a reduced trellis, cf. Fig. 12. The state reduction factor is equal to $r_f = M^{\kappa R_c}$. (Here, only such a first level state reduction is considered which corresponds to the choice $J_k = M^{\kappa R_c}$ for $1 \leqq k \leqq K - 1$ and $J_K = 1$ in [35]. The notation of [35] is however not applicable here. Only for schemes with very long frequency pulses or with a convolutional code having a high constraint length, a state reduction by DFSE at higher levels is useful [34].)

The actual substate within a hyperstate is uniquely determined by the optimum path which leads to this hyperstate. The signal element associated with a branch between hyperstates varies and is a function of the substate within the emerging hyperstate. Thus, a feedback of the past survivor decision is used for the selection of the actual signal elements associated with the branches within the reduced trellis so that the symbols on the top of the path-registers influence the metric calculations.

Because a final decision has to be made between paths entering a common hyperstate, the contribution due to the last interval before their real merger to their Euclidean distance is lost. Therefore, the square of the utilizable normalized minimum Euclidean distance $d_{\min}'^2$ ([1], [34]) is reduced by this loss. The butterfly condition guarantees that such premature decisions are made only between paths which would actually merge in the next step. Without this property, an uncontrolled error propagation would occur and the code corresponding to the reduced trellis would be catastrophic. Therefore, some remarks on this condition pertaining to CPM with phase-increment- (or

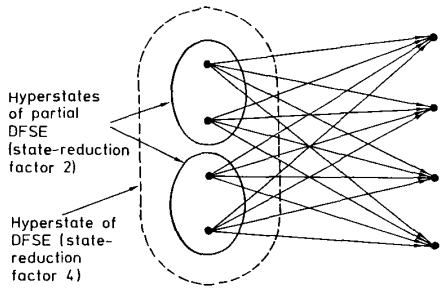

Fig. 12. Butterfly of a trellis with a 4-ary survivor decision (For DFSE all states of a butterfly form one hyperstate, for partial DFSE two hyperstates are defined).

frequency-)mapping are necessary. (For CPM with absolute or semidifferential phase-mapping, the inherent trellis encoder has a shift register memory so that DFSE is applicable at all state reduction levels.)

A) For CPM with partial response frequency pulses ($L \geqq 2$), DFSE is always applicable. This can be proved by observing that the nonrecursive part of the memory of the inherent trellis encoder of CPM (Fig. 1), which exists for $L > 1$, has a trellis with a butterfly structure. The next phase-state Ψ_{n-L+1} is not affected by the actual input symbols β_n [cf. (11)]. Thus, if two different memory-states have an identical successor state for one specific new input symbol β_n, path mergers exist for all new input symbols. The butterfly-structure of the nonrecursive part is incorporated into the overall trellis.

B) For $L = 1$ only schemes with $M \geqq p$ are considered, which have a fully interconnected phase-state trellis so that transitions between all states are possible in one step. The trellis consists of only one butterfly and therefore DFSE degenerates to a symbol-by-symbol detection with decision feedback. (DFSE can also be successfully applied to CPM ($L = 1$) combined with convolutional codes. In [34], some restrictions on convolutional encoders are derived to guarantee the butterfly property.)

Table III presents some results on the minimum normalized Euclidean distances which are utilizable by the reduced-state decoding procedure (row: DFSE), for 4-ary schemes with a smoothed frequency pulse of the type 3RC ([1]–[3]). The losses compared to a full state detection (FS) scheme are small, as the signal-elements of the last step before a merger of paths have small distances for these frequency pulses.

In Table IV, some examples of the combination of such 4-ary schemes ($h = 1/4$) with an additional rate $1/2$ convolutional encoder are presented (columns DFSE). In the columns labeled single trellis, the minimum utilizable Euclidean distances $d'^2_{\min}$ are listed for codes with equal coding and modulation intervals ($\kappa = 1$). The optimum codes have been given in [17], [34]. Additionally, Table IV contains results on double trellis coded CPM schemes with a mapping of the encoder output to the signal within two adjacent modulation intervals ($\kappa = 2$, [22]). The encoder structure pertaining to these schemes is shown in

TABLE III
COMPLEXITY NUMBER A, MINIMUM SQUARED EUCLIDEAN DISTANCES AND LOSSES DUE TO A REDUCTION IN STATES AND NUMBER OF LINEAR FILTERS. (M = 4-ary CPM-SCHEMES WITH FREQUENCY PULSES 3RC [1])

		h=1/4			h=1/3			h=1/2			h=3/4		
		A	d'^2_{min}	loss [dB]	A	d'^2_{min}	loss [dB]	A	d'^2_{min}	loss [dB]	A	d'^2_{min}	loss [dB]
all-dim	FS	128	0.96	0	96	1.67	0	64	3.36	0	128	5.36	0
	part. DFSE, rf=2	64	0.96	0	48	1.67	0	32	3.36	0	64	5.28	0.06
	DFSE, rf=4	32	0.95	0.04	24	1.65	0.05	16	3.10	0.34	32	4.56	0.70
	DFSE+part. Pre., rf=8	16	0.75	1.00	12	1.30	1.08	8	2.69	0.96	16	3.98	1.29
6-dim	FS	128	0.96	0	96	1.66	0.01	64	3.33	0.03	128	5.02	0.28
	part. DFSE, rf=2	64	0.96	0	48	1.66	0.01	32	3.33	0.03	64	4.96	0.33
	DFSE, rf=4	32	0.95	0.04	24	1.64	0.08	16	3.08	0.37	32	4.36	0.89
	DFSE+part. Pre., rf=8	16	0.75	1.00	12	1.29	1.10	8	2.67	0.99	16	3.85	1.43
4-dim	FS	128	0.94	0.09	96	1.60	0.18	64	3.12	0.32	128	3.06	2.50
	part. DFSE, rf=2	64	0.94	0.09	48	1.60	0.18	32	3.12	0.32	64	3.02	2.50
	DFSE, rf=4	32	0.93	0.14	24	1.58	0.24	16	2.90	0.63	32	2.39	3.50
	DFSE+part. Pre., rf=8	16	0.74	1.13	12	1.26	1.22	8	2.52	1.24	16	2.01	4.25

TABLE IV
OPTIMUM CONVOLUTIONAL ENCODERS AND SQUARED MINIMUM EUCLIDEAN DISTANCES AT THE STATE REDUCTION FOR SEVERAL VALUES OF THE COMPLEXITY NUMBER A). ($M = 4$, $h = 1/4$, 3RC)

A	single-trellis R_c=1/2 FS d'^2_{min}	single-trellis R_c=1/2 DFSE, rf=2 d'^2_{min}	double-trellis R_c=2/3·3/4=2/4 FS d'^2_{min} (X_0, X_1, X_2)	part. DFSE, rf=2 d'^2_{min} (X_0, X_1, X_2)	DFSE, rf=4 d'^2_{min} (X_0, X_1, X_2)	part. DFSE+ part. Pre., rf=4 d'^2_{min} (X_0, X_1, X_2)	DFSE+ part. Pre., rf=8 d'^2_{min} (X_0, X_1, X_2)
4	—	—	—	—	—	—	2.03 cf. FS, A=32
8	—	—	—	—	2.16 cf. FS, A=32	2.29 cf. FS, A=32	2.85 cf. DFSE, A=16
16	—	0.47	—	2.42 cf. FS, A=32	2.88 $\begin{pmatrix} D & 1+D^2 & 1 \\ D & 0 & 1 \end{pmatrix}$	3.28 cf. FS, A=64	3.20 $\begin{pmatrix} 0 & 1 & 0 \\ D^2 & 0 & 1+D+D^2 \end{pmatrix}$
32	0.48	2.85	2.42 $\begin{pmatrix} 0 & 1 & 0 \\ D & 0 & 1 \end{pmatrix}$	3.40 cf. FS, A=64	3.46 $\begin{pmatrix} 0 & 1 & 0 \\ D^2 & 0 & 1+D+D^2+D^3 \end{pmatrix}$	3.90 cf. FS, A=128	
64	2.86	3.06	3.40 $\begin{pmatrix} 0 & 1 & 0 \\ D & 0 & 1+D^2 \end{pmatrix}$	4.00 cf. FS, A=128			
128	3.07	3.54	4.00 $\begin{pmatrix} D & 1+D^2+D^3 & 1 \\ D & 0 & 1 \end{pmatrix}$				

Fig. 13. The rate $R_c = 2/4$ results from a convolutional encoder with rate $2/3$ and a redundant mapper with rate $3/4$, which forces a constant LSB x_0 at the modulator input over two modulation intervals. This implies a reduction in the number of phase-states at the boundaries of the coding interval $2T$ by a factor of two. The reference to the optimum codes in Table IV is related to the structure of Fig. 13. The most important result presented in Table IV, is the fact that a higher utilizable Euclidean distance is achieved at a given complexity number A, when a code with a greater constraint length is used together with a suboptimum decoding procedure, instead of a shorter code decoded by the full state algorithm. Especially at low complexity numbers, double trellis-coded schemes clearly exhibit superior performance compared to single trellis-coded schemes.

The problem of error propagation due to decision feedback was addressed by simulation with some of the results given in Figs. 17–19. (Additional results have been presented in [22], [34].) For all examples considered, only a small degradation occurred at moderate error rates ($\approx 10^{-3}$), while at low error rates ($< 10^{-4}$) almost no performance degradation was observed.

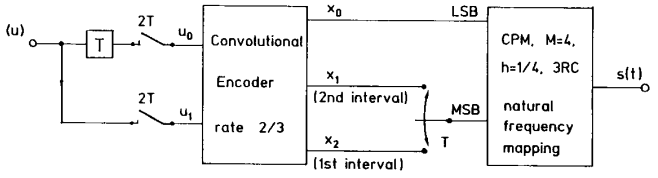

Fig. 13. Block diagram of the double trellis-coded 4-ary CPM schemes listed in Table IV.

The decrease in the utilizable Euclidean distance caused by the loss of the contribution of the last interval before a merger of paths, can be avoided by a less rigorous state reduction procedure. For schemes with $M^{\kappa R_c} \geqq 4$, not all states of a butterfly are combined to a hyperstate. According to [35], these states are partitioned into several classes which form the hyperstates. Fig. 12 illustrates such a state partitioning of a 4-ary butterfly into 2 hyperstates. This special case of reduced-state-sequence-estimation (RSSE) will be henceforth denoted by partial DFSE.

By a proper selection of the states which are combined to a hyperstate, it is possible in many cases to avoid minimum distance error events being truncated by this state reduction method [37]. Therefore, the complexity can be halved or even reduced at higher levels without any loss relative to the minimum Euclidean distance. As an example, the trellis of the scheme with $M = 4$, $h = 1/4$, $L = 1$ is drawn in Fig. 14 where one of the minimum distance error events has been displayed with bold face lines. None of these error events is truncated, if the phase-states $\Psi = 0$ and $\Psi = 2$ are combined to the first and the phase-states $\Psi = 1$ and $\Psi = 3$ to the second hyperstate, respectively.

The error events corresponding to $\beta = 0$ to $\beta = 2$, or $\beta = 1$ to $\beta = 3$ and vice versa which are shortened by one interval, have a greater distance than the minimum distance events. Therefore, no asymptotic SNR-loss results from this state reduction. A second advantage of this partial DFSE method is a reduction in the error propagation because the decision feedback is only less than $M^{\kappa R_c}$-ary.

Results for examples in which partial DFSE has been applied to CPM are presented in Tables III and IV together with the state reduction factor r_f in the rows or columns labeled part. DFSE. Simulation results are shown in Figs. 17 to 19. (In Figs. 18 and 19, results for part. DFSE are not distinguishable from those using full state detection.)

For symmetrical smoothed frequency pulses ($L \geqq 3$), the contribution to the Euclidean distance of the first interval after the path split in the encoder-modulator trellis, is as small as that contributed by the last step before their merger. Therefore, neglecting these distance portions offers the possibility of an additional state reduction. An illustration of this simplification method in Fig. 15 shows one butterfly of a trellis where the signal elements a_0 and a_1 as well as b_0 and b_1 which are associated to branches splitting at the states A and B, respectively, differ only slightly. Therefore, their arithmetic means $\tilde{a}$ and $\tilde{b}$, respectively, may be used as reference signal elements at the receiver. With this approximation no particular metric calculations and survivor decisions are necessary for the states C and D. For partial response CPM schemes, this procedure corresponds to the use of a simplified model of the inherent trellis encoder at the receiver [cf. Fig. 1 and (6)] where the influence of the actual input symbol β_n on the selection of a signal element is neglected. The signal table contains arithmetic means due to the neglected input β_n. Furthermore, the first delay element in Fig. 1 is no longer necessary for a state description of the simplified receiver and no further distinction of the states C and D in Fig. 15 is necessary when a delay element in the nonrecursive part of the trellis encoder is omitted. The intersymbol interference caused by neglecting a precursor of the fequency pulse cannot be controlled, and therefore intolerable losses occur for this rigorous state reduction method in the examples considered here (denoted by "Pre." in Figs. 18 and 19).

This disadvantage can be overcome by modifying this precursor neglect in a manner similar to the modification of DFSE to partial DFSE. For schemes with $M^{\kappa R_c} \geqq 4$, the branches which emerge from a state are partitioned into subsets in such a way that the maximum intrasubset Euclidean distance is minimal. (This partitioning is equivalent to the usual set partitioning [29], [35], however, with the inverse destination.) Each subset is represented at the receiver by the arithmetic mean of its elements. The state reduction factor equals the number of elements per subset. Fig. 16 shows an example of such a simplified model of the inherent trellis encoder of a 4-ary scheme used at the receiver with partial precursor neglect. The LSB of the actual phase-increment β_n has no influence on the reference signal element. One binary delay element (LSB β_n) is not necessary for the state description and therefore the number of states is halved. The unprocessed intersymbol interference due to this partial precursor neglect diminishes to a small amount so that only low losses have to be tolerated as evidenced by the results pertaining to the part. Pre. labeling of Tables III and IV, and Figs. 18 and 19.

In the chosen examples with smoothed frequency pulses 3RC and $M^{\kappa R_c} = 4$, a most interesting tradeoff between receiver complexity and distance loss exists for a full application of DFSE together with partial precursor neglect

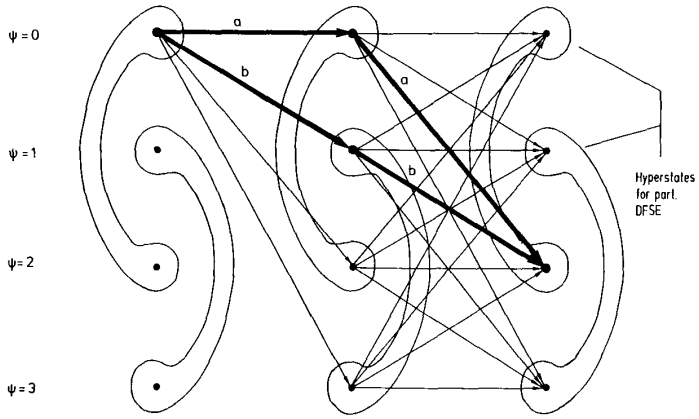

Fig. 14. Trellis of the scheme $M = 4$, $h = 1/4$, 1REC. Combination of states to hyperstates without a truncation of minimum distance error events (partial DFSE).

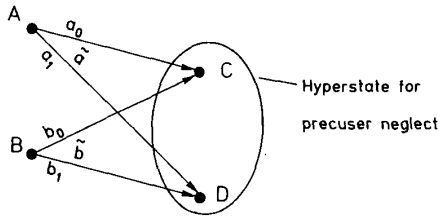

Fig. 15. Butterfly with slightly different signal elements for splitting branches.

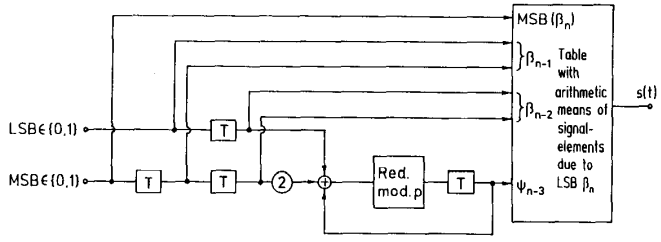

Fig. 16. Model of the inherent trellis encoder of a 4-ary CPM-scheme ($L = 3$) used at the receiver for a partial neglect (LSB) of a precursor of the frequency pulse (state reduction factor $r_f = 2$).

(DFSE + part. Pre.) where a state reduction factor of 8 is achieved at small SNR-losses. For $M^{\kappa R_c} > 4$ higher state reduction factors are also possible.

The application of RSSE and partial precursor neglect to CPM has to be compared to the search algorithm presented in [37]. This algorithm involves calculations of the metrics for all successors of a few active states. From these, the best paths are determined by a selection procedure in order to limit the number of active states after an identification of merging paths has been completed so as to avoid a multiple trace of identical paths. In [37], an example of a very successful application of this search algorithm to CPM is given, whereas a less propitious example can be found in [34]. The necessary number of active states appears to be almost insensitive to the total number of states. Consequently the state reduction method proposed here is advantageous for schemes with an originally moderately high number of states ($\leqq 128$). In Fig. 18, the results of simulating the search algorithm with $A = 8$ and $Z = 4$ active states are shown with a dotted line. The DFSE + part. Pre. method is clearly superior to the search algorithm for this complexity number. When $A = 16$, both algorithms perform approximately equally, however the RSSE algorithm has a more regular structure and at high data rates a parallel implementation is possible. Furthermore at the same number of active states this algorithm needs less operations than the search algorithm, especially for $M^{\kappa R_c} \leqq 4$. For schemes with a very high number of states, a more detailed comparison of both state reduction methods is necessary. (For the example pre-

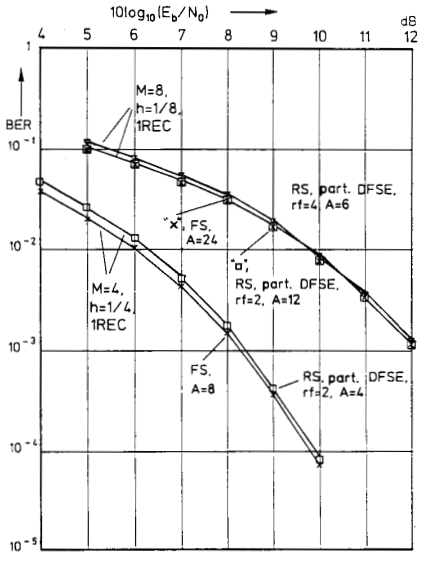

Fig. 17. Simulation results for 4- and 8-ary CPM-schemes ($h = 1/4$ and $h = 1/8$, 1REC), state-reduction by part. DFSE (6 dimensions, simulation up to at least 100 independent error events for each point).

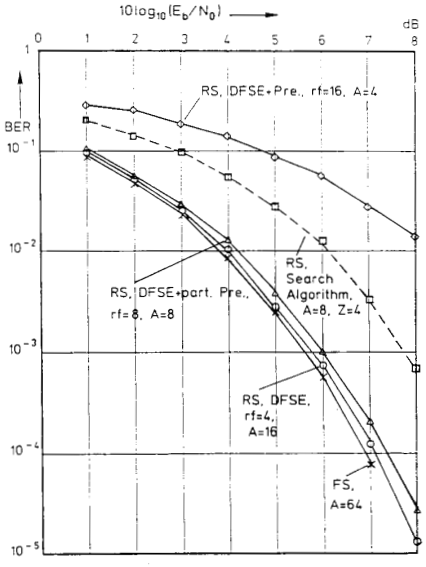

Fig. 18. Simulation results for several state-reduction procedures, $M = 4$, $h = 1/2$, $3RC$ (6 dimensions, simulation up to at least 100 independent error events for each point).

sented in [37] [$M = 8$; $h = 1/4$; 3RC, $Z = 256$], a reduction to 16 states is possible via DFSE + part. Pre., method, whereas 10 states are sufficient for the search algorithm.)

V. Conclusions

By separating both complexity problems, namely the number of linear filters and the number of memory-states required in optimum coherent CPM receivers, a straightforward procedure to reduce such complexity has been proposed and its usefulness evaluated in this paper. The reduction in the number of filters can be done more rigorously than the state-reduction at a given SNR-loss. The result yields a double or triple realization of complex baseband signal-processing associated with conventional quadrature PSK-/QAM-receivers. On the other hand, the construction of truly four-dimensional modulation schemes with a constant envelope that go beyond the CPM-schemes currently under discussion seems to be possible by a proper selection of reference signals while maintaining power and bandwidth efficiency features. The four or six dimensional receiver structure offers the implementation of open loop or decision-aided synchronization methods analogous to those discussed for trellis-coded PSK and QAM.

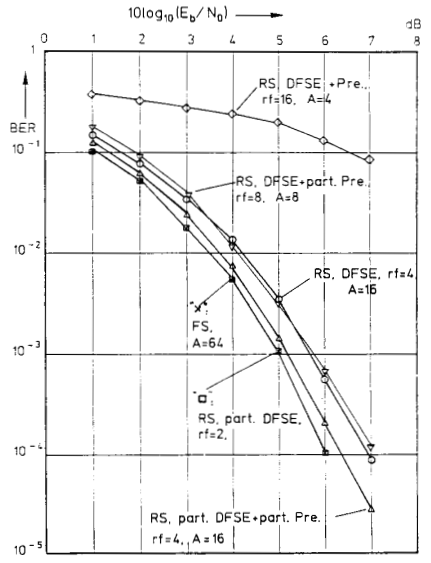

Fig. 19. Simulation results for a double trellis-coded CPM-scheme with redundant mapping (ref. to [22] and Table IV, $A = 64$), $M = 4$, $h = 1/4$, $3RC$ (6 dimensions, simulation up to at least 100 independent error events for each point).

The losses caused by incomplete processing of the nonlinear intersymbol interference in CPM-signals with smoothed frequency pulses are reduced by the use of decision feedback. Additional state reduction is demonstrated by the use of substitute signals at the receiver which are formed by the arithmetic mean of slightly different signal elements. This method allows an almost continuous tradeoff between receiver complexity-reduction and SNR-loss. The remaining state-numbers are comparable to those encountered in trellis-coded PSK and QAM, so that CPM with smoothed frequency pulses is useful at equivalent data rates with a similar detection effort.

Acknowledgment

The authors gratefully acknowledge the valuable suggestions and criticisms of the anonymous reviewers. The authors are greatly indebted to Prof. D. Bukofzer for his

careful reading and linguistic assistance in producing this paper.

REFERENCES

[1] J. B. Anderson, T. Aulin, and C. E. Sundberg, *Digital Phase Modulation*. New York: Plenum, 1986.

[2] T. Aulin, C. E. Sundberg, and N. Rydbeck, "Continuous phase modulation, parts I and II," *IEEE Trans. Commun.*, vol. COM-29, pp. 196–225, Mar. 1981.

[3] C. E. Sundberg, "Continuous phase modulation," *IEEE Commun. Mag.*, vol. 24, pp. 25–38, Apr. 1986.

[4] R. M. Gagliardi, *Satellite Communications*. New York: Van Nostrand Reinhold, 1984.

[5] S. J. Simmons and P. H. Wittke, "Low complexity decoders for bandwidth efficient digital phase modulation," *GLOBECOM '82*, Miami, FL, 1982, *Conf. Rec.*, pp. E 7.7.1–E 7.7.5.

[6] A. Svensson, C. E. Sundberg, and T. Aulin, "A class of reduced complexity Viterbi detectors for partial response continuous phase modulation," *IEEE Trans. Commun.*, vol. COM-32, pp. 1079–1087, Oct. 1984.

[7] T. Aulin, C. E. Sundberg, and A. Svensson, "MSK-type receivers for partial response continuous phase modulation," ICC '82, Philadelphia , PA, June 1982, *Conf. Rec.*, pp. 6F5.1–6F5.6.

[8] A. Svensson and C. E. Sundberg, "Serial MSK-type detection of partial response continuous phase modulation," *IEEE Trans. Commun.*, vol. COM-33, pp. 44–52, Jan. 1985.

[9] P. Galko and S. Pasupathy, "Linear receivers for generalized MSK," *Int. Conf. on Commun., ICC '82*, Philadelphia, PA, June 1982, pp. 6F5.1–6F5.6

[10] C. E. Sundberg and A. Svensson, "Parallel and serial MSK-type detection of partial response continuous phase modulation," *The 1983 Mediterranean Electrotech. Conf., MELECON '83*, Athens, Greece, *Conf. Rec.*, p. B8.01.

[11] J. M. Wozencraft and I. M. Jacobs, *Principles of Communication Engineering*. New York: Wiley, 1965.

[12] H. J. Landau and H. O. Pollak, "Prolate spheroidal wave functions, Fourier analysis and uncertainty-III: The dimension of the space of essentially time- and band-limited signals," *Bell Syst. Tech. J.*, vol. 41, no. 4, pp. 1295–1336, July 1962.

[13] P. M. Dollard, "On the time-bandwidth concentration of signal functions forming given geometric vector configurations," *IEEE Trans. Inform. Theory*, vol. IT-10, pp. 328–338, Oct. 1964.

[14] A. Duel and C. Heegard, "Delayed decision-feedback sequence estimation," presented at the Allerton Conf., Commun. Contr. Comput., Oct. 1985.

[15] M. V. Eyuboglu and S. U. Qureshi, "Reduced-state sequence estimation with set partitioning and decision feedback," *GLOBECOM '86*, Houston, TX, 1986, *Conf. Rec.*, vol. 2, pp. 29.2.1–29.2.6.

[16] W. L. Liu, "Faltungscodierung für Modulationsverfahren mit kontinuierlicher Phase," Diplomarbeit, Tech. Univ. Munich, July 1986.

[17] J. Huber and W. L. Liu, "Convolutional codes for CPM using the memory of the modulation process," *GLOBECOM '87*, Tokyo, Japan, 1987, *Conf. Rec.*, vol. 3, pp. 43.1.1–43.1.5.

[18] B. E. Rimoldi, "A decomposition approach to CPM," *IEEE Trans. Inform. Theory*, vol. 34, pp. 260–270, Mar. 1988.

[19] K. L. Chung, *Markov Chains with Stationary Transition Probabilities*, 2nd ed. Berlin: Springer-Verlag 1967.

[20] I. B. Anderson and D. P. Taylor, "A bandwidth-efficient class of signal space codes," *IEEE Trans. Inform. Theory*, vol. IT-24, pp. 703–712, Nov. 1978.

[21] L. E. Franks, "Carrier and bit synchronization in data communication—A tutorial review," *IEEE Trans. Commun.*, vol. COM-28, pp. 1107–1121, Aug. 1980.

[22] J. Huber and W. L. Liu, "Double trellis-coded CPM," *ICC '88*, Philadelphia, PA, 1988, *Conf. Rec.*, pp. 51.4.1–51.4.6.

[23] D. Dzung, "Optimum CPM waveforms," *ICC '87*, Seattle, WA, 1987, *Conf. Rec.*, pp. 20.6.1–20.6.5.

[24] B. E. Rimoldi, "Design of coded CPFSK modulation systems for bandwidth and energy efficiency," submitted to *IEEE Trans. Commun.*

[25] G. Lindell, C.-E. Sundberg, and T. Aulin, "Minimum Euclidean distance for combinations of short rate 1/2 convolutional codes and CPFSK modulation," *IEEE Trans. Inform. Theory*, vol. IT-30, pp. 509–519, May 1984.

[26] S. V. Pizzi and S. G. Wilson, "Convolutional coding combined with continuous phase modulation," *IEEE Trans. Commun.*, vol. COM-33, pp. 20–29, Jan. 1985.

[27] G. Ascheid, Y. Chen, and H. Meyr, "Synchronization, Demodulation und Dekodierung bei bandbreiteneffizienter Übertragung," *NTZ Archiv*, Bd. 4, H.12, pp. 355–363, Dez. 1982.

[28] P. Y. Kam, "Maximum likelihood carrier phase recovery for linear suppressed-carrier digital data modulations," *IEEE Trans. Commun.*, vol. COM-34, pp. 522–527, June 1986.

[29] G. Ungerboeck, "Trellis-coded modulation with redundant signal sets—Parts I and II," *IEEE Commun. Mag.*, vol. 25, pp. 5–21, Feb. 1987.

[30] L.-F. Wei, "Trellis-coded modulation with multidimensional constellations," *IEEE Trans. Inform. Theory*, vol. IT-33, pp. 483–501, July 1987.

[31] G. D. Forney, "The Viterbi algorithm," *Proc. IEEE*, vol. 61, pp. 268–278, Mar. 1973.

[32] F. L. Vermuelen and M. E. Hellmann, "Reduced-state Viterbi decoding for channels with intersymbol interference," *ICC'74*, Minneapolis, MN, June 1974, *Conf. Rec.*, pp. 37B-1–37B-4.

[33] W. Sauer and W. Rupprecht, "Ein aufwandsgünstiges suboptimales Detektionsverfahren für stark verzerrte und gestörte Datensignale," *NTZ Archiv*, Bd. 9, 1987, H.7, pp. 155–169.

[34] J. Huber and W. L. Liu, "Reduced-state-Viterbi-detection of CPM combined with convolutional codes," in *Proc. SITA '87*, vol. 2, Enoshima, Japan, Nov. 1987, pp. ED 2-2-1–ED 2-2-6.

[35] M. V. Eyuboglu and S. U. Qureshi, "Reduced-state sequence estimation with set partitioning and decision feedback," *IEEE Trans. Commun.*, vol. COM-36, pp. 13–20, Jan. 1988.

[36] J. L. Massey, "The how and why of channel coding," in *Proc. 1984 Int. Zürich Sem. Digital Commun.*, Zürich, Switzerland, 1984, pp. E 1.1–E 1.7.

[37] T. Aulin and T. Larsson, "Two classes of algorithms for asymptotically optimal simplified MLSD with application to digital radio," *EUROCOM '88*, Stockholm, Sweden, 1988, *Conf. Rec.*, D.3.6, pp. 110–113.

[38] A. Premji and D. P. Taylor, "Receiver structures for multi-*h* signaling formats," *IEEE Trans. Commun.*, vol. COM-35, pp. 439–451, Apr. 1987.

[39] ——, "A practical receiver structure for multi-*h* CPM," *IEEE Trans. Commun.*, vol. COM-35, pp. 901–908, Sept. 1987.

Johannes Huber (M'87) was born in Hausham, Bavaria, West Germany, in 1951. He received the Dipl.-Ing. degree in electrical engineering from the Technical University Munich in 1977.

From 1977 to 1982 he was a Research Assistant at the Institute for Communication Engineering of the University of the Federal Armed Forces, Munich from which he received the Dr.-Ing. degree with a thesis on coding for channels with memory. Since 1982 he is an Assistant Professor at this University. His research interests are coding theory, modulation schemes, high rate baseband data transmission and algorithms for signal detection and adaptive equilization for channels with severe intersymbol interference. In 1988, he received the research award from the German Informationstechnische Gesellschaft.

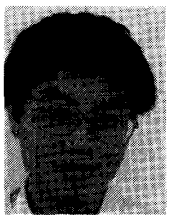

Weiling Liu (S'87) was born in Shanghai, People's Republic of China, in 1959. He received the Dipl.-Ing. degree in electrical engineering from the Technical University Munich, West Germany, in 1986.

Since Oct. 1986 he has been a Research Assistant at the Institute for Communication Engineering of the University of the Federal Armed Forces and is currently working for a Dr.-Ing. dissertation. His research interests are bandwidth and power efficient coding and modulation.